Monthly Notices
of the
ROYAL ASTRONOMICAL SOCIETY

MNRAS **454,** 3912–3919 (2015) doi:10.1093/mnras/stv2150

Old age and supersolar metallicity in a massive $z \sim 1.4$ early-type galaxy from VLT/X-Shooter spectroscopy⋆

I. Lonoce,[1,2]† M. Longhetti,[1] C. Maraston,[3] D. Thomas,[3] C. Mancini,[4] A. Cimatti,[5] F. Ciocca,[1,2] A. Citro,[5] E. Daddi,[6] S. di Serego Alighieri,[7] A. Gargiulo,[5] R. Maiolino,[8] F. Mannucci,[7] M. Moresco,[5] L. Pozzetti,[5] S. Quai[5] and P. Saracco[1]

[1]*INAF–Osservatorio Astronomico di Brera, via Brera 28, I-20121 Milano, Italy*
[2]*Dipartimento di Scienza e Alta Tecnologia, Università degli Studi dell'Insubria, via Valleggio 11, I-22100 Como, Italy*
[3]*Institute of Cosmology and Gravitation, University of Portsmouth, Dennis Sciama Building, Burnaby Road, Portsmouth PO1 3FX, UK*
[4]*INAF–Osservatorio Astronomico di Padova, Vicolo dell'Osservatorio 5, I-35122 Padova, Italy*
[5]*Dipartimento di Fisica e Astronomia, Università di Bologna, Viale Berti Pichat 6/2, I-30127 Bologna, Italy*
[6]*CEA-Saclay, Service d'Astrophysique, F-91191 Gif-sur-Yvette, France*
[7]*INAF—Osservatorio Astrofisico di Arcetri, Largo Enrico Fermi 5, I-50125 Firenze, Italy*
[8]*Kavli Institute for Cosmology, University of Cambridge, Madingley Road, Cambridge CB3 0HA, UK*

Accepted 2015 September 15. Received 2015 September 7; in original form 2015 May 19

ABSTRACT

We present the first estimate of age, *stellar* metallicity and chemical abundance ratios, for an individual early-type galaxy at high-redshift ($z = 1.426$) in the COSMOS (Cosmological Evolution Survey) field. Our analysis is based on observations obtained with the X-Shooter instrument at the Very Large Telescope (VLT), which cover the visual and near-infrared spectrum at high ($R > 5000$) spectral resolution. We measure the values of several spectral absorptions tracing chemical species, in particular magnesium and iron, besides determining the age-sensitive D4000 break. We compare the measured indices to stellar population models, finding good agreement. We find that our target is an old ($t > 3$ Gyr), high-metallicity ([Z/H] > 0.5) galaxy which formed its stars at $z_{\rm form} > 5$ within a short time-scale $\sim$0.1 Gyr, as testified by the strong [α/Fe] ratio ($>$0.4), and has passively evolved in the first $>$3–4 Gyr of its life. We have verified that this result is robust against the choice and number of fitted spectral features, and stellar population model. The result of an old age and high-metallicity has important implications for galaxy formation and evolution confirming an early and rapid formation of the most massive galaxies in the Universe.

Key words: galaxies: elliptical and lenticular, cD – galaxies: high-redshift – galaxies: stellar content.

1 INTRODUCTION

The cosmic history of galaxy mass assembly represents one of the open key questions in cosmology. Early-type galaxies (ETGs) are the most effective probes to investigate this topic, as they are the most massive and oldest galaxies in the local Universe and most likely those whose stars formed earliest. Observations have shown that a population of massive and passive galaxies is already in place at high redshift, when the Universe was only a few Gyr old (Cimatti et al. 2004; Saracco et al. 2005). So far, the main physical parameters related to their formation and assembly have been mainly estimated on local ETGs, and their ageing and evolution can mix up and confuse the original properties when the bulk of their mass formed and assembled. Information on the star formation (SF) time-scale of high-z ETGs can be obtained from the detailed chemical abundance ratios of their stellar populations (Thomas, Maraston & Bender 2005), which can be derived by a detailed spectral analysis. Indeed, the abundance of Iron with respect to α-elements is tightly correlated with the time delay between Type I and Type II supernovae (SN), giving a direct probe of the time-scale within which SF has occurred.

Up to now, only few works have experimented a spectral analysis on ETGs at $z > 1$ (Onodera et al. 2012; Jørgensen et al. 2014; Lonoce et al. 2014) due to the low S/N of the available spectroscopic data, and they were mostly focused on age estimates, in particular using

⋆ Based on observations collected at the European Organization for Astronomical Research in the Southern hemisphere, Chile (programme: 086.A-0088(A))

† E-mail: ilaria.lonoce@brera.inaf.it

the *UV* region (Cimatti et al. 2008). The analysis of the rest-frame optical spectrum is still lacking.

Furthermore, measures are usually performed on stacked spectra (Onodera et al. 2015), thus deleting possible peculiarities of single objects.

A single-object measurement of age, stellar metallicity and chemical abundance ratios of $z > 1.2$ ETGs is missing at the present time. We fill this gap, presenting the first attempt to measure the detailed chemical composition, besides age, of a $z \sim 1.4$ ETG directly in the early stages of its evolution.

Throughout this paper, we assume a standard cosmology with $H_0 = 70$ km s^{-1} Mpc^{-1}, $\Omega_m = 0.3$ and $\Omega_\Lambda = 0.7$.

2 COSMOS-307881: SPECTROSCOPIC DATA

Our target is a bright and massive ($>10^{11}$ $M_\odot$) ETG from the K-selected galaxy catalogue in the COSMOS (Cosmological Evolution Survey) field (McCracken et al. 2010). It is one of the 12 galaxies with K_s(Vega) <17.7 selected by Mancini et al. (2010) on the basis of three criteria: (i) non-detection at 24 μm in the *Spitzer*+MIPS data (Sanders et al. 2007); (ii) visual elliptical morphology (see Fig. 1, top panel); (iii) multicolour Spectral Energy Distribution (SED) consistent with old and passive stellar populations with no dust reddening. All available information are shown in Table 1. For further details see Mancini et al. (2010) and Onodera et al. (2012).

From these studies we can infer that our target is an old and slightly compact ($R_e \sim 0.3\ R_c^{z=0}$, w.r.t. the local size-mass relation) ETG, and most of its mass is composed by a passively evolving stellar population. In the following we present a new analysis of the stellar population properties of this ETG based on new spectroscopic data, which, thanks to the high resolution in a wide spectral range of the X-Shooter spectrograph, allows us to measure the stellar metallicity of this high-z target.

Spectroscopic observations were carried out with the X-Shooter spectrograph on the Very Large Telescope (VLT)/UT2 (Vernet et al. 2011) in Italian guaranteed time during the nights 2011 February 9–10, (programme: 086.A-0088(A)). The target has been observed under bad sky condition (seeing >2 *arcsec*) during the first night (about 1.7 h for the VIS and UVB arms and about 1.9 h for the NIR arm), while during the second night more than 4 h of exposure have been collected under good sky conditions (seeing ∼0.8 *arcsec*). We decided to consider only the latter set of observations. The use of the 1.0 arcsec slit in the UVB arm and 0.9 arcsec slit in the VIS and NIR arms, resulted in a spectral resolution of 5100, 8800 and 5600 in the UV, VIS and NIR, respectively.

The data reduction has been performed taking advantage of the ESO pipeline (Goldoni et al. 2006) regarding the first steps of the process, and completed by means of `IRAF` tools. In Fig. 1 the reduced mono-dimensional spectrum of 307881 (black line) is shown in comparison with the photometric points (cyan diamonds, from Muzzin et al. 2013; McCracken et al. 2012). Overlaid is a 4 Gyr, supersolar metallicity ($Z = 0.04$) simple stellar population (SSP) model of Maraston & Strömbäck (2011, M11) based on the MILES stellar library (Sánchez-Blázquez et al 2006, red line). Note that this template is the most similar in term of age and total metallicity, to the best-fitting solution that will be derived in the next section. The full spectral model, as known, does not include the α/Fe parameter (see Maraston & Strömbäck 2011), which we shall derive using selected absorption-line models in the next section (see Thomas, Maraston & Johansson 2011).

The original high resolution of the spectrum (e.g. ∼1 Å in the VIS) has been decreased to match the lower resolution of the models (i.e. ∼2.54 Å at rest-frame, and ∼6 Å in the VIS at $z = 1.4$), which are used to perform the analysis of spectral indices (for details see Lonoce et al., in preparation). Note that we adopted the MILES-based M11 models instead of the higher resolution ones (M11-ELODIE or M11-MARCS, see http://www.maraston.eu/M11) to take advantage of the increasing S/N in downgrading the observed resolution. The value of the signal to noise ratio (S/N) obtained in the spectral region around 5000 Å restframe is ∼7 per pixel.

In Fig. 2 we show how the H β and Mg_b are expected to appear on a synthetic template (upper first panel) that broadly reproduces the observed one. The model is first adapted to the measured velocity dispersion (upper second panel), then downgraded to be as noisy as the observed spectrum (upper third panel) and finally compared to the observed one (bottom panel). The similarity between expected and observed absorption features is quite evident.

3 SPECTRAL ANALYSIS

As a first step, we measured the redshift of 307881 fitting the Mg_b line region, which is the cleanest from the background residuals, as it can be seen in Fig. 1 (bottom panel), finding $z = 1.426 \pm 0.001$. The Mg_b line region has been also used to find a best-fitting velocity dispersion estimate, that resulted to be $\sigma = 385 \pm 85$ km/s. More details on the fitting procedure adopted to fix both z and σ will be described in the forthcoming paper.

We then selected some indices whose absorption features are clearly visible in the observed spectrum, to try to simultaneously derive both the mean age and the metallicity of its stellar population. The selected indices are: D4000 index (Hamilton 1985), $H\gamma_F$ (Worthey & Ottaviani 1997), G4300, Fe4383, Ca4455, Fe4531, H β, Fe5015 and Mg_b (Lick/IDS system, Worthey et al. 1994). In particular, it is well known that the Mg_b index is the best *metallicity* and *chemical abundance* dependent index in the region around 5000 Å restframe (Korn, Maraston & Thomas 2005). In Table 2 we report the measured values of these indices together with their errors derived by means of *Monte Carlo* simulations set on the uncertainties in the flux measurements.

Finally, we want to point out the presence of the [OII]3727 emission line (Fig. 1, middle panel). We can exclude that its origin is due to an active AGN, since we do not see any other signature in the observed wide spectral window. There are reasonable possibilities that this emission is caused by the UV ionizing emission of old stars in post-main-sequence phases (Yi & Yoon 2004), as confirmed by UV indices (Lonoce et al., in preparation), while a strong contribution from SF can be excluded. Indeed, as it can be noted from Fig. 2 (left-hand panels), it is highly unlikely that the H β feature is affected by emission, considering also that its value suggests a stellar population age in good agreement with that derived by the H γ and D4000 index.

4 MODEL COMPARISON

In Fig. 3 we show the observed Mg_b and H β indices (blue diamond), compared to the predictions of the SSP of Thomas et al. (2011; hereafter TMJ models), based on the MILES library for a wide range of ages (from 0.1 Gyr shown up to the age of the Universe at $z \sim 1.4$, i.e. 4 Gyr); supersolar metallicities [Z/H] = 0.35 (red lines) and [Z/H] = 0.67 (cyan lines), and various α/Fe parameters, namely [α/Fe] = 0.0, 0.3, 0.5. Models assume a Salpeter (1955) initial mass

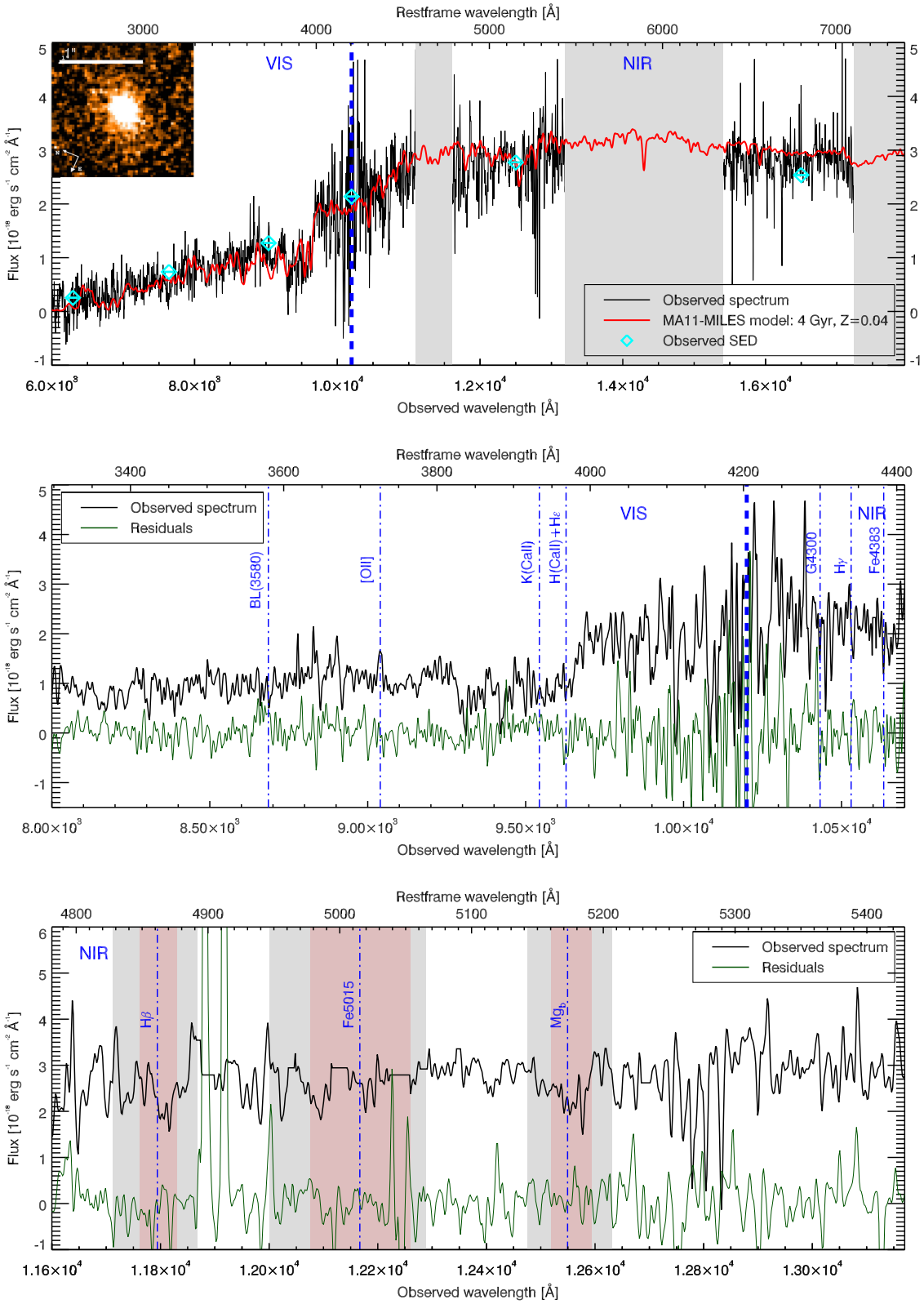

Figure 1. COSMOS 307881. The galaxy observed spectrum (black line) is compared to a model (Maraston & Strömbäck 2011) with age of 4 Gyr and supersolar metallicity ($Z = 0.04$), and to observed photometric data (cyan diamond). Top panel: VIS and NIR spectral region together with the *HST*/ACS *I*-band image of the target. Middle panel: zoom of the 4000 Å rest-frame region. Bottom panel: zoom of the 5000 Å restframe region. The main absorption (and one emission) lines in each spectral region are highlighted. Dark green lines indicate the residual spectrum.

Table 1. COSMOS-307881. Data derived from the analysis of Onodera et al. (2012): *K*-band magnitude in Vega system (K_s); spectroscopic redshift (z_{spec}^{ONOD}); stellar population age (Age_{phot}) and logarithm of the stellar mass ($\log\mathcal{M}_*$) derived from SED fitting assuming a Chabrier IMF (Chabrier 2003); effective radius (R_e); degree of compactness ($C=R_e/R_{e,\,z=0}$); Sérsic index (*n*). Units of right ascension are hour, minutes and seconds, and unites of declination are degrees, arcminutes and arcseconds.

ID	RA	DEC	K_s (Vega)	z_{spec}^{ONOD}(*)	Age_{phot} (Gyr)	$\log\mathcal{M}_*$ ($M_\odot$)	R_e (kpc)	*C*	Sérsic *n*
307881	10:02:35.64	02:09:14.36	17.59	1.4290 ± 0.0009	3.50	11.50	2.68 ± 0.12	0.32	2.29 ± 0.10

Note. (∗)This work: $z_{spec} = 1.426 \pm 0.001$.

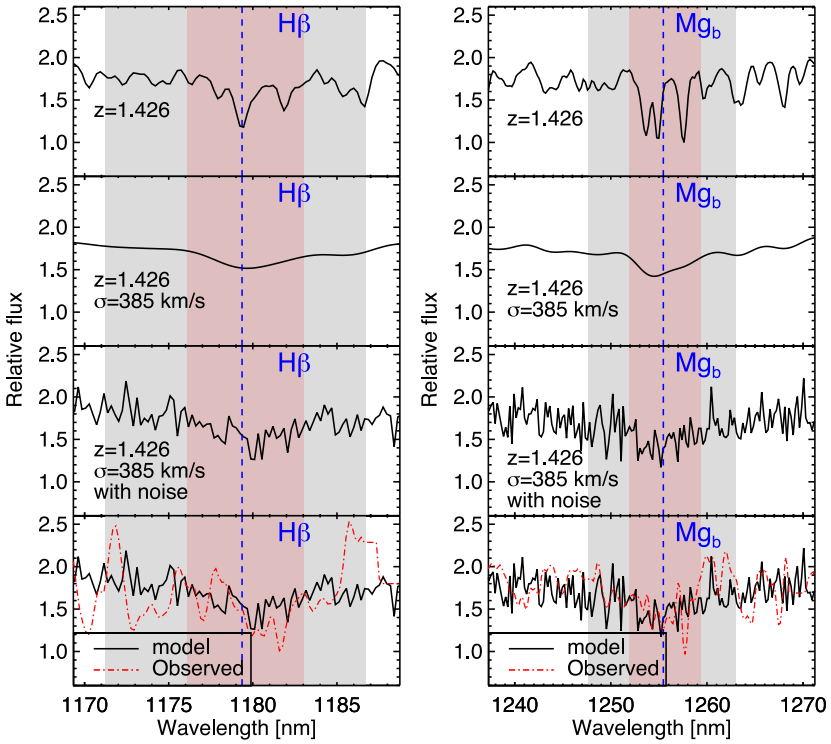

Figure 2. H β (left-hand panels) and Mg_b (right-hand panels) features in the 4 Gyr, 2 Z⊙ metallicity model shown in Fig. 1. From top to bottom we show: model at $z \sim 1.4$; model corrected for $\sigma = 385$ km/s; model downgraded for the observed Poissonian noise; model compared to the observed spectrum (point-dashed red line).

Table 2. Measured indices values.

Index	value
D4000	2.44 ± 0.12
D_n4000	2.42 ± 0.17
$H\gamma_F$	-1.56 ± 0.92
G4300	6.52 ± 1.12
Fe4383	7.40 ± 1.74
Ca4455	1.06 ± 0.83
Fe4531	3.20 ± 1.40
H β	2.52 ± 0.93
Fe5015	3.89 ± 1.91
Mg_b	5.75 ± 0.81

function (IMF), and are corrected for the measured velocity dispersion value of $\sigma = 385 \pm 85$ km/s. As it can be seen, the extreme value of the Mg_b index fully requires high-metallicity models up to [Z/H] = 0.67. In particular, in Fig. 3 the model expectations for these indices are reported also in case of non-solar values of the α-enhancement [α/Fe], from 0.3 to 0.5 (dashed and dotted lines, respectively).

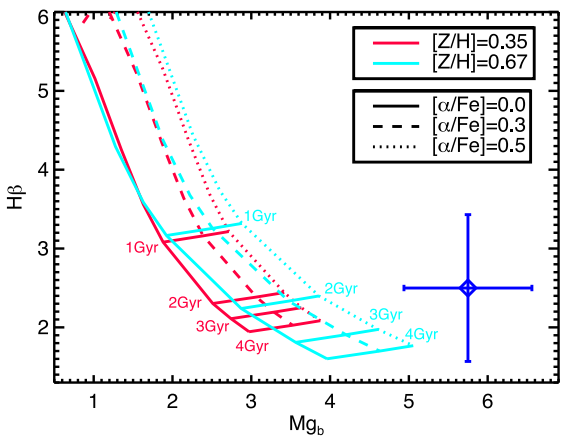

Figure 3. H β versus Mg_b plot. Comparison between the measured indices (blue diamond) and models of Thomas et al. (2011) (lines). Ages run from 0.1 to 4 Gyr, for super solar metallicities of [Z/H] = 0.35, 0.67 (red, cyan lines), and α-element abundances: [α/Fe] = 0.0, 0.3, 0.5 (solid, dashed, dotted lines). The models are corrected for the measured value of $\sigma = 385$ km/s.

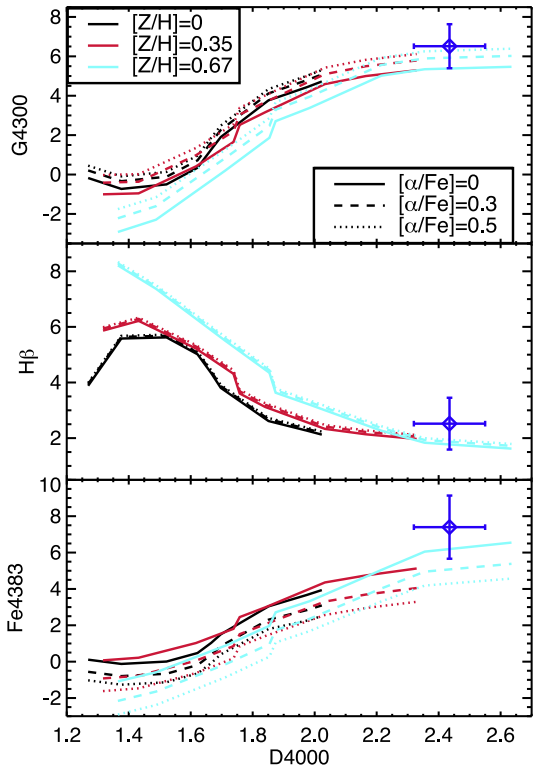

Figure 4. Comparison between four measured indices (G4300, Hβ and Fe4383 versus D4000) and the models of Thomas et al. (2011). Ages run from 0.1 − 4 Gyr, metallicities from [Z/H] = 0, 0.35, 0.67 (black, red, cyan lines), and α-element abundances from [α/Fe] = 0, 0.3, 0.5 (solid, dashed, dotted lines). The measured values are shown with a blue diamond. Indices values of models are corrected for the measured value of σ = 385 km/s.

Models corresponding to extreme values of [α/Fe]>0.5 seem to be required to match the observations.

The behaviour of the Mg_b index, requiring such extreme values of Z, is confirmed also when considering the other absorption lines that we were able to measure on this X-Shooter spectrum. Indeed, as it can be noticed in Fig. 4 where we propose three examples of Lick indices (G3400, Hβ and Fe4383, upper, middle and bottom panel, respectively) as a function of D4000, all measured indices consistently point towards a very-high metallicity ([Z/H] ∼ 0.67, cyan lines) being only marginally consistent with the 2 $Z_\odot$ values ([Z/H] ∼ 0.35, red lines).

Notice that the highest metallicity models in Thomas et al. (2011) are partly in extrapolation, as they are sampling the edge of the parameter space in terms of the available empirical fitting functions for such extreme stellar parameters (see Johansson, Thomas & Maraston 2010). At the same time, the underlying stellar tracks are based on real calculations (see Maraston et al. 2003, for details).

More quantitatively, we have computed the best-fitting solution obtained comparing all 9 observed indices values (Table 2) with models. The free parameters were age (0.1–4.5 Gyr, truncated at the age of Universe, with step 0.1 Gyr),[1] the total metallicity (from [Z/H]=−2.25 to [Z/H] = 0.67, with step 0.01) and the α/Fe-enhancement (from [α/Fe]=−0.3 to [α/Fe] = 0.5, with step 0.01). The minimum χ^2 value corresponds to an age of $4.0^{+0.5}_{-0.8}$ Gyr, metallicity [Z/H] = $0.61^{+0.06}_{-0.05}$ and [α/Fe] = $0.45^{+0.05}_{-0.19}$, with χ^2 = 0.7 and an associated probability ∼70 per cent. Errors indicate the range values of these parameters over all the solutions associated with probabilities larger than 65 per cent. The distributions of the three fitting parameters, displayed in different χ^2 ranges, are shown in Fig. 5, top panel. A global picture of the χ^2 values can be seen in Fig. 6 where the minimum χ^2 trends of the three parameters of all solutions are shown. It is easy to notice that ages <2 Gyr can be completely excluded due to the rapid increasing of their χ^2 values towards younger ages. Instead for ages >4.5 Gyr (limit of the Universe age, not shown here) the χ^2 values remains practically constant.

Furthermore, we found that models with $Z \leq Z_\odot$ provide a fit of the free parameters with a probability less than 0.1 per cent.

We also verified the strength of this result by repeating the same fitting process selecting smaller and different set of indices, finding very similar solutions with respect to the previous ones based on the whole set of indices. Two examples are shown in Fig. 5 (middle and bottom panels): the distributions of the fitting solutions are obtained from two smaller sets of indices (i) D4000, G4300, Hγ, Fe4383, Hβ, Fe5015 and Mg_b and (ii) D4000, Hγ, Hβ and Mg_b) which lead to a best-fitting solution of (i) age = 4.0 Gyr, [Z/H] = 0.61 and [α/Fe] = 0.44 with χ^2 = 0.9, and (ii) age = 4.0 Gyr, [Z/H] = 0.60 and [α/Fe] = 0.5 with χ^2 = 0.5, both totally consistent with the all-indices one.

We also evaluated the feasibility of this analysis on this low S/N spectrum, in particular for metallicity and α-enhancement estimates, by repeating it on a set of 500 mock spectra built on a model spectrum with parameters as the best fit to the observed one (cf. Table 3) and downgraded with the Poissonian observed noise. The obtained distributions of the measured [Z/H] and [α/Fe] are shown in Fig. 7. They all peak around the true original values (red vertical lines) demonstrating that within the declared errors the obtained values are solid.

Furthermore we tested if the large error on the velocity dispersion could affect the results by performing the same analysis assuming σ = 300 km/s. We found the same best-fitting solution (4.1 Gyr, [Z/H] = 0.6, [α/Fe] = 0.41 with χ^2 = 0.6).

Finally, in order to test the model dependence of this result, we repeated the same analysis adopting the Bruzual & Charlot (2003) models (BC03). These models do not include the [α/Fe] parameter, hence we shall use them to constrain age and total metallicity solely. The BC03 models cover a slightly lower Z range with respect to our fiducial TMJ models, and are based on different stellar evolutionary tracks. The BC03 best-fit corresponds to an age of 4.5 Gyr and a metallicity of [Z/H] = 0.4, which is the maximum available metallicity in these models. Hence our result of a high-age and high-Z is not model dependant.

It is important to note the high metallicity is mainly derived as a consequence of the maximum allowed age of 4.5 Gyr. Should we allow the age to be older than the age of the Universe, the metallicity will decrease, as a result of age/metallicity degeneracy. Actually, the large error bar of both the indices and of σ prevents a real precise measure of the metallicity, but the peculiarity of such a strong Mg_b absorption band combined with the narrow range of possible ages (due to its redshift), make necessary the assumption of a very high value of the stellar metallicity.

[1] Note that we have performed the analysis using all available model ages (up to 15 Gyr) thereby ignoring the age of the Universe as a constrain. However, as no particular improvement was noticed in the derived quantities, we decided to focus on ages within the age of the Universe at $z \sim 1.4$.

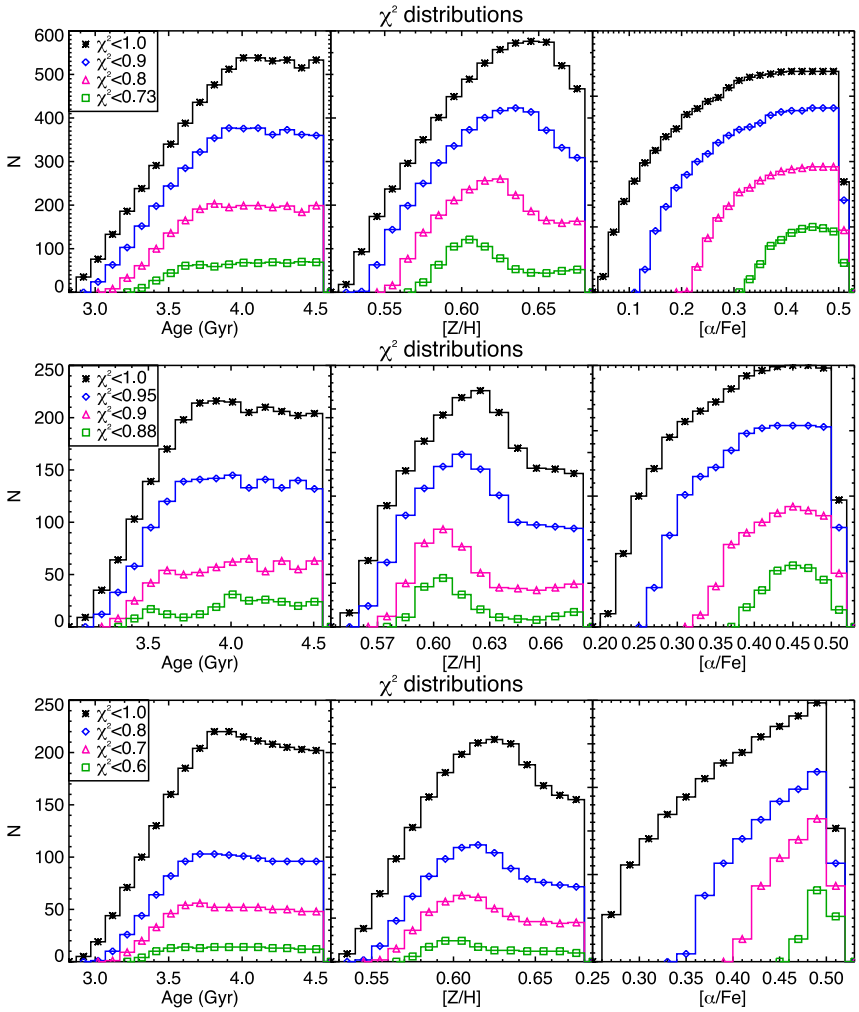

Figure 5. Distributions of the fitting-solutions: age, metallicity and α-enhancement. Colours and symbols indicate solutions in different χ^2 ranges, e.g. green squares include the most probable solutions. Top panel: distributions obtained from the all-indices analysis; middle panel: distributions obtained from a smaller set of indices: D4000, G4300, Hγ, Fe4383, Hβ, Fe5015 and Mg$_b$; bottom panel: distributions obtained from a smaller set of indices: D4000, Hγ, Hβ and Mg$_b$.

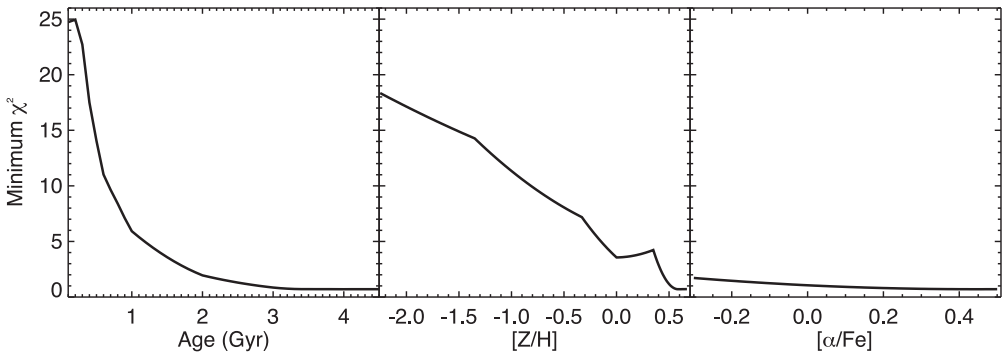

Figure 6. Trends of minimum χ^2 for age, [Z/H] and [α/Fe] of all obtained solutions. In particular, ages <2 Gyr can be completely excluded due to the rapid degrade of χ^2 towards younger ages.

5 DISCUSSION AND CONCLUSIONS

We have performed a detailed spectroscopic analysis of a z=1.426, massive ($M^* \sim 10^{11}$M$_\odot$), early-type galaxy. We gain strong evidence of a high-stellar metallicity and α-enhancement, and old (relative to its redshift) age (Table 3). These quantities constrain the past SF history experienced by the galaxy. In particular, the [α/Fe] ratio, quantifying the time delay between Type II SN events, responsible of the production of α-elements, and the Type Ia SNs, related to the formation of Fe-peak elements, allows us to determine the SF time-scale (Thomas et al. 2005). The high value [α/Fe] ∼0.4 obtained for 307881 is a direct signature that its SF time-scale

Table 3. Results: spectroscopic redshift (z_{spec}) and velocity dispersion (σ) obtained from this spectroscopic analysis; best-fitting values of age (Gyr), [Z/H] and [α/Fe].

z_{spec}	σ (km/s)	Age (Gyr)	[Z/H]	[α/Fe]
1.426 ± 0.001	385 ± 85	$4.0^{+0.5}_{-0.8}$	$0.61^{+0.06}_{-0.05}$	$0.45^{+0.05}_{-0.19}$

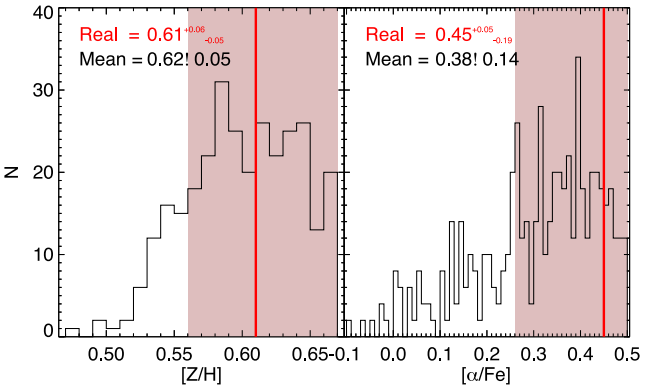

Figure 7. Distributions of [Z/H] and [α/Fe] derived for a set of 500 mock spectra built on a model spectrum with parameters (Table 3) as those of the best-fit to the observed spectrum and adding the Poissonian noise. The two distributions are well peaked around the true original values (red vertical lines).

must have been short. In particular, adopting the simple theoretical modelling of Thomas et al. (2005), where the SF is modelled with a Gaussian function, we obtain a time-scale Δt $\sim$0.1 Gyr covering the interval within which 95 per cent of the stars were formed. Considering also the old age of its stellar content, this suggests that 307881 formed the bulk of its stars at $z_{\rm form} > 5$ within a short time-scale of Δt $\sim$0.1 Gyr and then passively evolved over the following 4 Gyr.

With the high [α/Fe] value suggesting a short SF time-scale for 307881, the clear indication for an extremely high total metallicity opens new issues on the gas enrichment history of the Universe. It is worth emphasizing that the global integrated metallicity of the local ETGs never reaches values higher than the 1–2 $Z_{\odot}$. Indeed, we considered the local sample analysed in Thomas et al. (2010) and quickly verified that the metallicity and [α/Fe] values of 307881 together with its velocity dispersion estimate, are not included in the local distribution of values, even if such high values of Z and [α/Fe] are expected for dense ETGs as suggested by these scaling relations. Thus, this suggests that this galaxy must experience mass accretion events (minor merging) from $z = 1.4$ to $z = 0$ which will move it on the observed local scaling relations towards lower values of both Z and σ, diluting the extreme metallicity stars and confining them in the central part of the galaxy. Indeed, such extreme metallicity values are in some cases found in the inner core of local massive ETGs (Trager et al. 2000; Thomas et al. 2005; Martín-Navarro et al. 2015) which are known to show metallicity gradients (La Barbera et al. 2012). We calculated that adding e.g. 15 per cent of a sub-solar metallicity component, as in the case of dwarf galaxies, to 307881 would decrease the measure of its average metallicity to the local observed values. On the other hand, the gas metallicities up to now measured in $z > 3$ star-forming galaxies result to be solar or sub-solar, and do not match at all the high stellar value measured in our target galaxy (Mannucci et al. 2009) and in the centres of local ETGs (Spolaor et al. 2008). It is out of the aims of the present paper to suggest a possible explanation of this missing detection of high-z high-metallicity gas. A possibility is that the lower gas metallicity comes from dilution through infalling primeval gas, or selective mass-loss of metals in galactic winds. At the same time, the estimate of the metallicity of the Broad Line Regions in quasars at $z > 4$ reveals gaseous metallicities even higher than the stellar one reported here (Juarez et al. 2009), suggesting the possibility that their enriched gas is involved in the initial SF events of (at least some) high-z massive protoelliptical galaxies.

ACKNOWLEDGEMENTS

We are grateful to the anonymous referee for helpful comments on our manuscript. We kindly thank Francesco La Barbera for his precious help in the data reduction and Kyle Westfall for helpful discussions. IL acknowledges the institute of Cosmology and Gravitation of the University of Portsmouth for a brilliant research visit during which a larger part of this project was worked out. IL, ML, AG and PS acknowledge the support from grant Prin-INAF 2012-2013 1.05.09.01.05. AC, LP, MM acknowledge the support from grant PRIN MIUR 2010-2011. CM and DT acknowledge The Science, Technology and Facilities Council for support through the Survey Cosmology and Astrophysics consolidated grant, ST/I001204/1.

REFERENCES

Bruzual G., Charlot S., 2003, MNRAS, 344, 1000
Chabrier G., 2003, PASP, 115, 763
Cimatti A. et al., 2004, Nature, 430, 184
Cimatti A. et al., 2008, A&A, 482, 21
Goldoni P., Royer F., François P., Horrobin M., Blanc G., Vernet J., Modigliani A., Larsen J., 2006, Proc. SPIE, 6269, 626933
Hamilton D., 1985, ApJ, 297, 371
Johansson J., Thomas D., Maraston C., 2010, MNRAS, 406, 165
Juarez Y., Maiolino R., Mujica R., Pedani M., Marinoni S., Nagao T., Marconi A., Oliva E., 2009, A&A, 494, L25
Jørgensen I., Chiboucas K., Toft S., Bergmann M., Zirm A., Schiavon R., Grutzbauch R., 2014, AJ, 148, 117
Korn A., Maraston C., Thomas D., 2005, A&A, 438, 685
La Barbera F., Ferreras I., de Carvalho R. R., Bruzual G., Charlot S., Pasquali A., Merlin E., 2012, MNRAS, 426, 2300
Lonoce I., Longhetti M., Saracco P., Gargiulo A., Tamburri S., 2014, MNRAS, 444, 2048
McCracken H. J. et al., 2010, ApJ, 708, 202
McCracken H. J. et al., 2012, A&A, 544, 156
Mancini C. et al., 2010, MNRAS, 401, 933
Mannucci F. et al., 2009, MNRAS, 398, 1915
Maraston C., Strömbäck G., 2011, MNRAS, 418, 2785
Maraston C., Greggio L., Renzini A., Ortolani S., Saglia R. P., Puzia T. H., Kissler-Patig M., 2003, MNRAS, 400, 823
Martín-Navarro I., La Barbera F., Vazdekis A., Ferré-Mateu A., Trujillo I., Beasley M. A., 2015, MNRAS, 451, 5600
Muzzin A. et al., 2013, ApJS, 206, 8
Onodera M. et al., 2012, ApJ, 755, 26
Onodera M. et al., 2015, ApJ, 808 161
Salpeter E. E., 1955, ApJ, 121, 161
Sánchez-Blázquez P. et al., 2006, MNRAS, 371, 703
Sanders D. B. et al., 2007, ApJS, 172, 86
Saracco P. et al., 2005, MNRAS, 357, 40
Spolaor M., Forbes D. A., Proctor R. N., Hau G. K. T., Brough S., 2008, MNRAS, 385, 675
Thomas D., Maraston C., Bender R., 2005, ApJ, 621, 673

Thomas D., Maraston C., Schawinski K., Sarzi M., Silk J., 2010, MNRAS, 404, 1775
Thomas D., Maraston C., Johansson J., 2011, MNRAS, 412, 2183
Trager S. C., Faber S. M., Worthey G., González J. J., 2000, ApJ, 119, 1654
Vernet J. et al., 2011, A&A, 536A, 105
Worthey G., Ottaviani D., 1997, ApJS, 111, 377
Worthey G., Faber S. M., González J. J., Burstein D., 1994, ApJS, 94, 687
Yi S. K., Yoon S., 2004, Ap&SS, 291, 205

This paper has been typeset from a TEX/LATEX file prepared by the author.